Research Article

Space Science Journal

Ionosonde Data Analysis for Precise Study of Ionospheric Electron Density

Amsalu Hundesa[1,2*]

[1]*College of Science, Department of Physics, Washera Geospace and Radar Science Research Laboratory (WaGRL), Bahir Dar University, P.O.Box 79, Ethiopia*

[2]*College of Science, Department of Physics, Bonga University, Bonga, Ethiopia*

***Corresponding Author**
Amsalu Hundesa, College of Science, Department of Physics, Washera Geospace and Radar Science Research Laboratory (WaGRL), Bahir Dar University, P.O.Box 79, Ethiopia

Submitted: 2024, Feb 02; **Accepted:** 2024, Feb 26; **Published:** 2024, Mar 21

Citation: Hundesa, A. (2024). Ionosonde Data Analysis for Precise Study of Ionospheric Electron Density. *Space Sci J, 1*(1), 01-12.

Abstract

The ionosphere, crucial for communication, navigation, and space weather forecasting, profoundly impacts our technological infrastructure by reflecting and refracting radio waves. Enter Ionosound, a cutting-edge ionospheric sounder system revolutionizing our ability to capture and analyze ionospheric data. Unlike traditional radar, Ionosound employs sound waves to probe electron density profiles, unlocking new insights into the ionosphere's intricate dynamics. This paper delves into Ionosound's principles, capabilities, and applications in studying electron density, showcasing its pivotal role in advancing atmospheric research and space weather prediction. With a focus on electron density profiles peaking between 150-350 km, we examine Ionosonde measurements capturing reflections from the E-layer to the F2 peak, with notable absorption observed in the D-layer below the E-layer. We leverage key ionospheric parameters such as electron density profile (Ne), maximum electron density (NmF2), maximum ionization height (hmF2), and critical frequency (foF2) to deepen our analysis. However, it's important to acknowledge Ionosonde's limitation in probing only the lower ionospheric region, prompting us to supplement our findings using the Chapman electron density profile to extend observations to upper layers. Through meticulous analysis, Ionosound empowers scientists to explore the ionosphere's responses to diverse phenomena with unprecedented precision, shaping the future of atmospheric science and space exploration.

Keywords: Ionospheric Measurement, Ionosound (Ionogram), Vertical Electron, Density

1. Introduction

The vertical-incidence ionosonde stands as a pinnacle of advanced technology, offering a sophisticated radar system tailored to penetrate and explore the ionosphere directly above it (Forsythe et al., 2021). Emitting concise bursts of radio energy vertically, this innovative apparatus meticulously analyzes the reflected signals to decipher the ionosphere's intricate characteristics. Through the modulation of carrier frequency, the ionosonde adeptly probes the diverse layers of the ionosphere, providing invaluable insights into its composition and behavior (McNamara et al., 2008).

Central to its operation is the precise recording of time delays between transmission and reception of radio pulses. This meticulous analysis serves as the cornerstone for scientists, enabling them to unravel the complex structure and dynamics of the ionosphere (Bilitza, 2008). Such understanding is pivotal for deciphering phenomena like radio wave propagation and space weather, with implications spanning communication, navigation, and atmospheric science (Ma et al., 2005). As an indispensable tool, the vertical-incidence ionosonde contributes significantly toscientific research andpractical applicationsin telecommunications and navigation (Chartier et al., 2012).

In the realm of atmospheric science, the ionosphere holds immense importance for comprehending various phenomena crucial to communication, navigation, and space weather forecasting. Emerging as a revolutionary technology in ionospheric measurement, Ionosound offers unparalleled capabilities in capturing and analyzing ionospheric data with precision and depth (Tsai et al., 2009). Harnessing advanced signal processing and analysis methods, Ionosound provides unique insights into the ionosphere's electron density profile through sound wave propagation, setting it apart from conventional radar systems (Garcıa-Fernández et al., 2003). With its ability to capture real-time ionospheric variations, Ionosound facilitates improved space weather monitoring and forecasting, crucial for mitigating adverse impacts on satellite communications, GPS navigation, and power distribution systems (Forsythe et al., 2021). Ground based ionosonde is still the basic tool for studying the bottom side electron density distribution (Rishbeth and Garriott, 1969). The ionosphericdensityprofilemeasureduptotheflayerpeak using ionosonde is defined as bottom side and is widely available due to global network of ionosondes (Warrington et al., 2012). But the part of the density profile above the F layer is not accessible to the ionosondes and can be measured only by Incoherent Scatter Radar (ISR),Topside sounders and Chapman functions to estimate the topside profile (Di Giovanni and Radicella,

1990; Stankov et al., 2003). The Chapman function offers a simple yet potent tool for analyzing ionospheric profiles, as demonstrated by studies such as (Huang and Reinisch, 2001). Reinisch et al. (2004) and Belehaki et al. (2003) have reported that the Chapman function, even when employing a constant scale height, accurately fits the topside ionospheric profile up to several hundred kilometers above the F2-peak. They sought to leverage bottom-side ionosonde data to extrapolate the variation in topside ionospheric density. Their method hinges on the approximation that the scale height above the peak of the F2 layer remains constant and equals the Chapman scale height at the height of the F2 layer peak density (hmF2) (Horwitz et al., 1990). By employing this constant scale height, they successfully reconstructed the topside profile.

This paper delves into the principles, capabilities, and applications of Ionosound technology in studying ionospheric electron density, advancing our understanding of ionospheric physics, and enhancing atmospheric modeling efforts. It also explores the challenges and future prospects associated with Ionosound data analysis, shaping the future of atmospheric science and space exploration. Additionally, this project aims to utilize ionosonde measurements, employing testing instruments to generate ionograms that provide further insights into the ionosphere's characteristics using Chapman function.

2. Data and Methodology

2.1 Ionosonde

The ionosonde is an instrument that measures the electron density profile of the ionosphere through the emissionofpulses(echoes) ofverticalelectromagneticenergy in relation to the ground. These echoes are recorded by the ionosondes and organized according to the frequency of transmission and the height of reflection of the electromagnetic pulses to form the so-called ionograms (Yamashita, 1999). A range of ionospheric parameters can be extracted from ionogram analysis. The parameter containing the layer E, and the layer F, include F1 or F2 in their names; a last group, containing neither of the letters E and F, provide information independent of ionosphericlayers. Anionosonde isahigh frequency(HF)radar used for ionospheric observations and probing. Ionosonde measurements utilize the fact that each plasma has a characteristic plasma frequency fp, which depends only on the electron density Ne of the plasma:

$$Ne/m^{-3} = 1.24 \times 10^{10}(fp/MHZ)^2 \qquad (1)$$

Ionosonde is the device to sound the ionosphere by radio waves so as to monitor the ionosphere characteristics. By varying the carrier frequency of pulses, typically from 1 to 30 MHz, the time delay at different frequencies is recorded (Barona Mendoza et al., 2017). The flight time of the radio wave between the transmission and reception at a particular frequency is the basic quantity that can be measured by the ionosonde and it provides an indication of the height of reflection. For vertical sounder, the height of reflection (virtual height, hv) of the ionosphere is estimated by the relation, which is given by

$$h_v = C\frac{\Delta t}{2} \qquad (2)$$

Since the radio wave propagates with speed that is different from the speed of light in vacuum, the height from equation 2 is not the true height. Ionosonde results are usually displayed as virtual height against band of frequency, which is known as ionogram. Actual reflection heights are smaller than virtual heights due to the ionospheric refraction effect. The Earth's magnetic field splits the echo trace into an ordinary and an extraordinary trace. The usual ionogram reduction techniques use only the ordinary trace. Parameters routinely deduced from ionograms include the plasma frequencies and virtual heights of the F and E peaks foF2 O stands for ordinary trace, foF1, foE, $h'F2$, hE. In addition the maximum usable frequency (MUF) is scaled from ionograms. MUF(3000) is the highest frequency that, refracted in the ionosphere, can be received at a distance of 3000 km. The propagation factor

$$M(3000)f2 = \frac{MUF}{fof2} \qquad (3)$$

The F2 layers peak height hmf2 is the F2 peak electron density height(km) computed using

$$hmf2 = \frac{1490}{M(3000)F2} - 176 \qquad (4)$$

As the signals moves up in frequency, it start to be reflected to the ground by the E-region and delay in receiving the pulse enables the approximation height to determine the ionospheric parameters for the operation of HF. The limitation of the ionosonde is that it can not prob the topside of the ionosphere above the F2 -peak. That means if you increases the frequency of the transmitter beyond the F2-layer the radio waves will not reflected but it will be transmitted. The trace around 100km is the Elayer and foE is the critical frequency of E-layer and $h'E$ is the virtual height of E-layer (Souza and Camargo, 2019).

2.2 Chapman Production Function

Production at maximum can never be larger than for an overhead Sun, and it increasing with zenith angle.The the profile decreases very rapidly with height below the altitudeofpeakproduction. Thebelowequationisthefinal form of Chapman function (Fang et al., 2016).

$$Q = q_{m,0}exp\left[-secXexp\left(-\frac{z - z_{m,0}}{H}\right)\right] \qquad (5)$$

3. Result and Discussion

In this paper ionogram measurements along with derived electron density height profile, form ionosonde in- stalled in Addis Ababa Ethiopia sations for the year 2014, may 27, 29 and 30 are seen in Fig 1, 2, 3, 4, 5, 6,7 and 8 respectively. Ionogram measurement Fig. (1a, 2a), Electron Density Profile Fig. (1b, 2b), peak electron density Fig. (1c, 2c) and virtual height Fig. (1d, 2d) on May 27 at 11:40:06 and and 12:00:06 UT respectively. In the ionogram measurement around two reflection heights are observed at different frequencies. Similary

Ionogram measurementFig. (3a, 4a), Electron Density Profile Fig. (3b,4b), peak electron density Fig. (3c, 4c) and virtual height Fig. (3d, 4d) on May 29 at 14:35:06 and and 15:10:05 UT respectively. Finally Ionogram measurement Fig. (5a, 6a), Electron Density Profile Fig. (5b, 6b), peak electron density Fig. (5c, 6c) and virtual height Fig. (5d, 6d) on May 30 at 14:35:06 and and 15:10:05 UT respectively. The Earth's ionosphere has been monitored since the 1930s by means of ionosondes that are radar transmitting vertically pulses of frequency usually between 0.1-30MHZ. As we can see from the figures the signals reflected as function of the frequency in what is called the ionogram. Fig. (7a) is the Chapman profile electron density used to probe the upper part of ionosphere electron density and the Fig. (7b) is shows us the absorbed electron density at D-layer and also the maximum electron density (Nmf_2) is around 380km, above this km the incoherent.

scatter radar, coherent scatter radar and Chapman profile are used to probe the ionosphere as well as ionospheric parameters. The 3rd plot tell us the critical frequency of E-layer (foE), critical frequency of F1-layer (fof_1) and the critical frequency of F2-layer (fof_2).

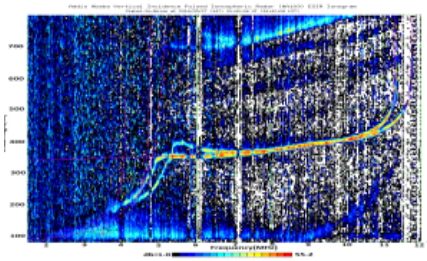

(a)

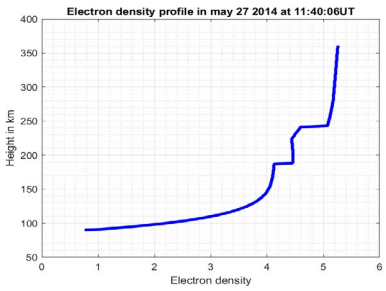

(b)

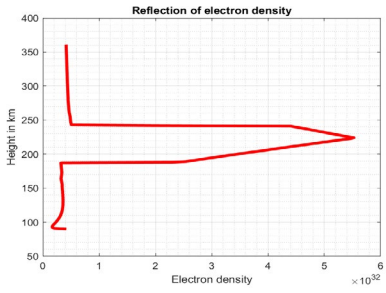

(c)

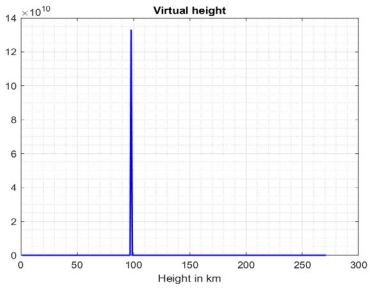

(d)

Figure 1: (a) Ionosonde Measurements displayed as virtual height against band of frequency, which is known as ionogram, (b) Electron Density Profile obtained from Ionosonde data, (c) Reflected electron density at F_2 peak and (d) virtual height on May 27 at 11:40:06 UT respectively.

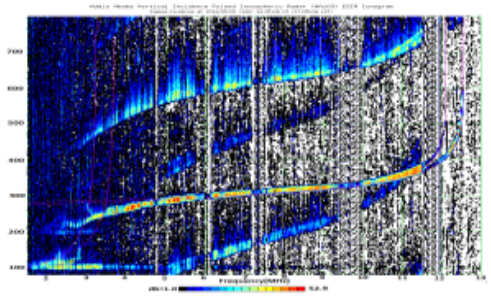

(a)

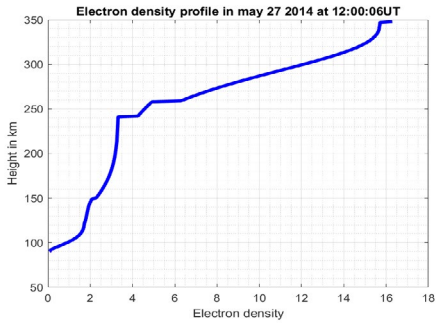

(b)

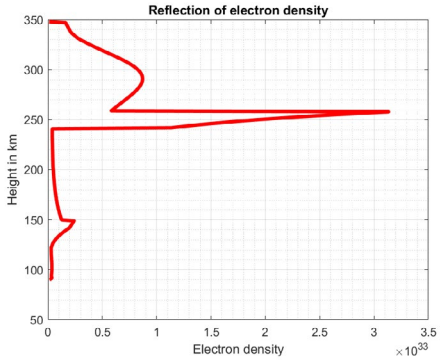

(c)

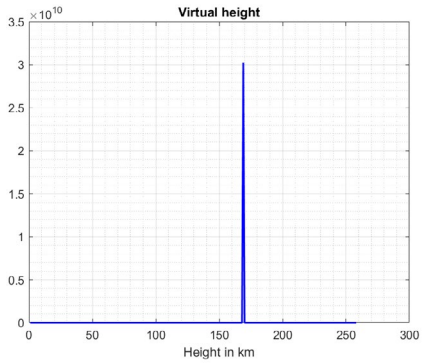

(d)

Figure 2: (a) Ionosonde Measurements displayed as virtual height against band of frequency, which is known as ionogram, (b) Electron Density Profile obtained from Ionosonde data, (c) Reflected electron density at F_2 peak and (d) virtual height on May 27 at 12:00:06 UT respectively.

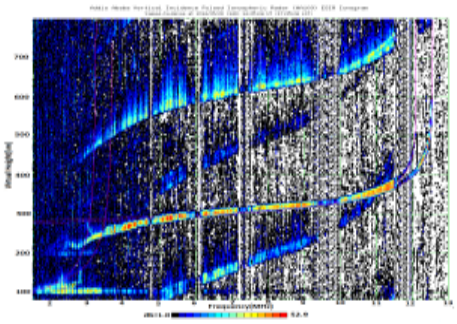

(a)

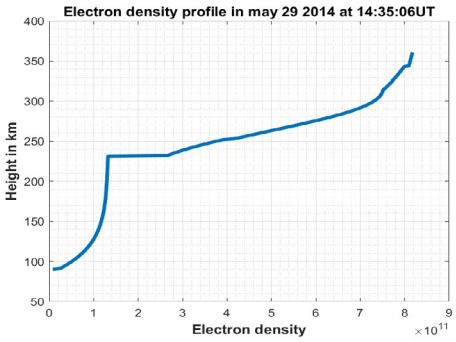

(b)

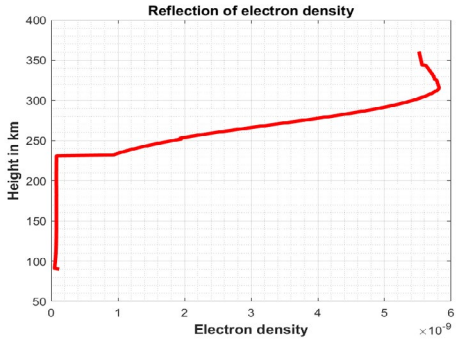

(c)

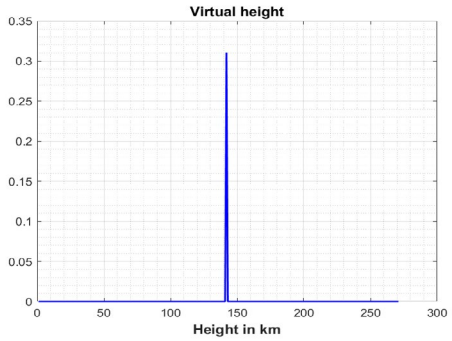

(d)

Figure 3: (a) Ionosonde Measurements displayed as virtual height against band of frequency, which is known as ionogram, (b) Electron Density Profile obtained from Ionosonde data, (c) Reflected electron density at F_2 peak and (d) virtual height on May 29 at 14:35:06 respectively.

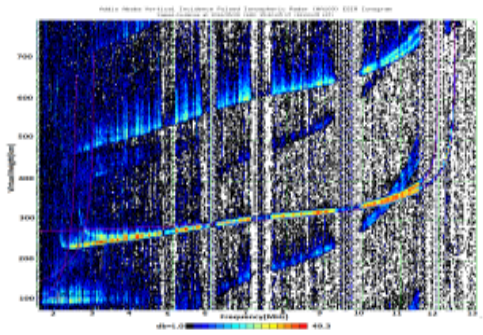

(a)

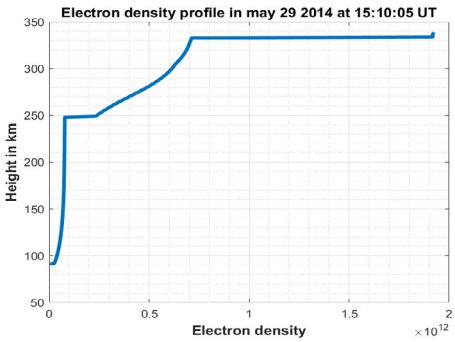

(b)

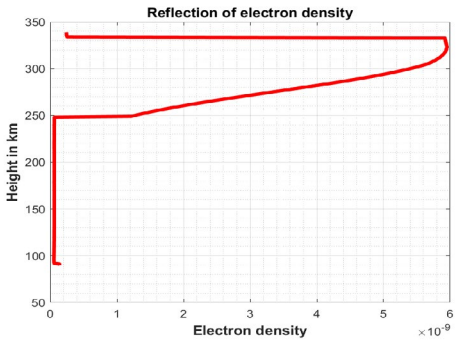

(c)

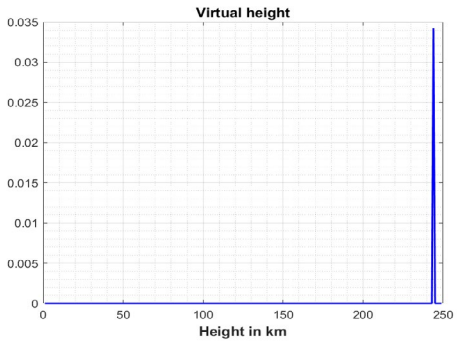

(d)

Figure 4: (a) Ionosonde Measurements displayed as virtual height against band of frequency, which is known as ionogram, (b) Electron Density Profile obtained from Ionosonde data, (c) Reflected electron density at F_2 peak and (d) virtual height on May 29 at 15:10:05 UT respectively

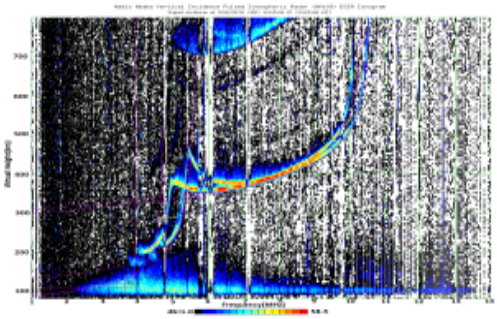

(a)

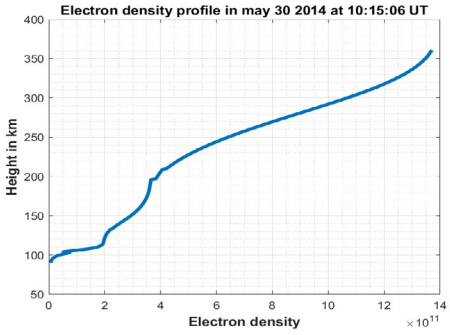

(b)

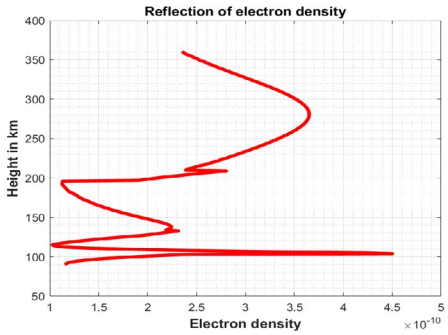

(c)

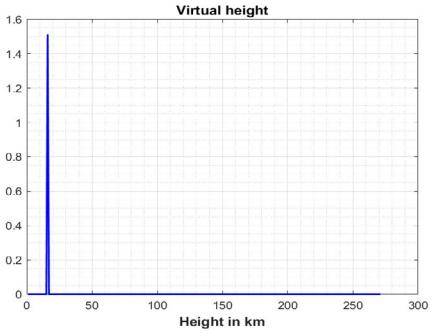

(d)

Figure 5: (a) Ionosonde Measurements displayed as virtual height against band of frequency, which is known as ionogram, (b) Electron Density Profile obtained from Ionosonde data, (c) Reflected electron density at F_2 peak and (d) virtual height on May 30 at 10:15:06 UT respectively

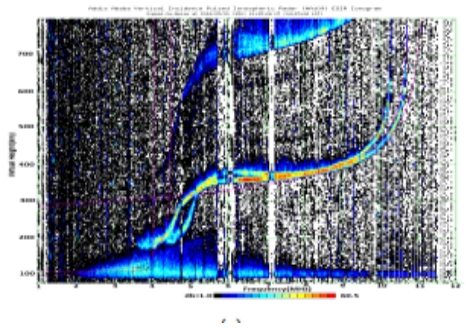

(a)

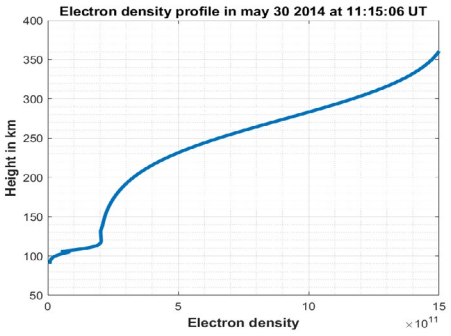

(b)

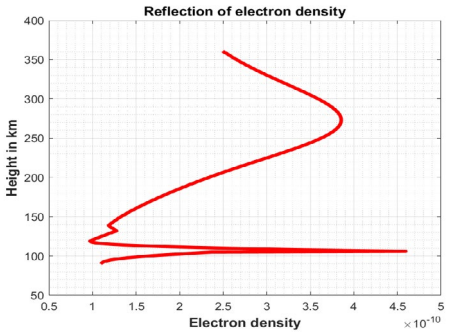

(c)

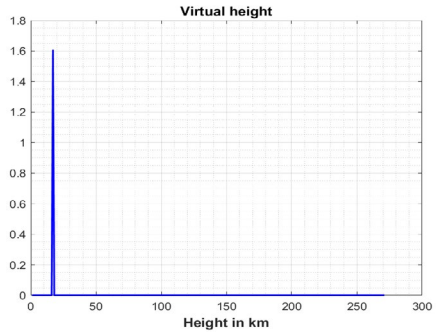

(d)

Figure 6: (a) Ionosonde Measurements displayed as virtual height against band of frequency, which is known as ionogram, (b) Electron Density Profile obtained from Ionosonde data, (c) Reflected electron density at F_2 peak and (d) virtual height on May 30 at 11:15:06 UT respectively

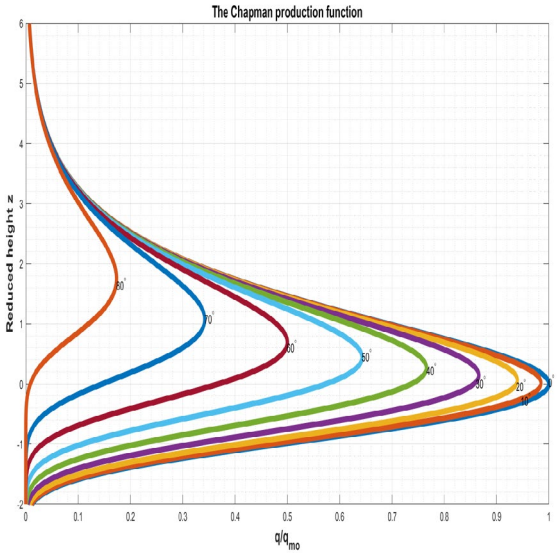

(a)

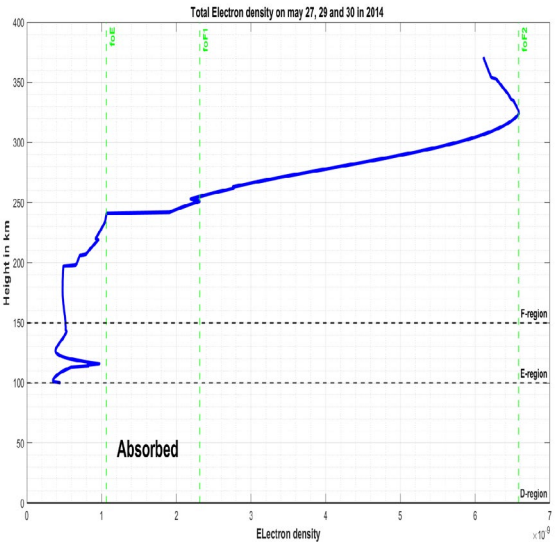

(b)

Figure 7: Comparison between the Chapman funcation model data and the vertical electron density distribution recorded by Ionosonde at Addisa Abab station in 2014 for three day in May.

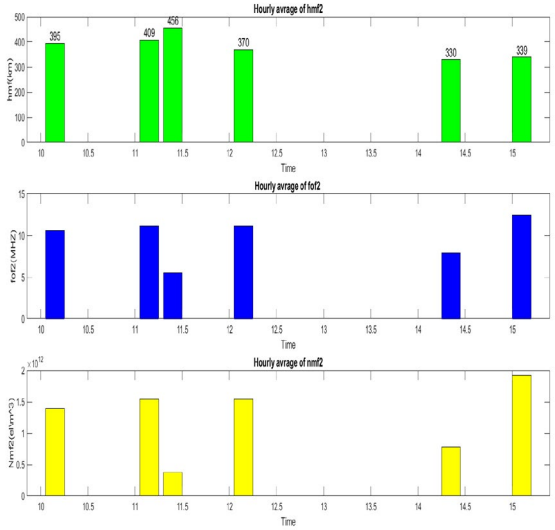

(a)

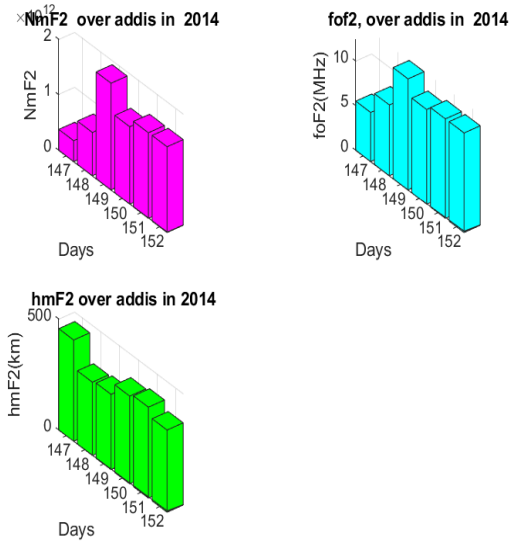

(b)

Figure 8: (a) Hourly mean of hmf2, fof2 and nmf2 values and (b) daily mean of Nmf2, fof2 and hmf2 values respectively.

The bottom side electron density of the ionosphere is measured using ionosunde measurements. The top side electron density is estimated by Chapman electron density profile. Ground based ionosonde is still the basic tool for studying the bottom side electron density distribution. The ionospheric density profile measured up to the F layer.

peak using ionosonde is defined as bottom side and is widely available due to global network of ionosondes. But the part of the density profile above the F layer is not accessible to the ionosondes and can be measured only by Incoherent Scatter Radar (ISR) or topside sounders aboard satellites. The topside sounder data is available only for a limited time period as there has been no current satellites mission carrying any topside sounder. Therefore,

Day	Time	hmF2	fof2	NmF2
27	11:40:06UT	456	5.5	0.3754E+12
27	12:00:06UT	348	11.46	0.1629E+13
29	14:35:06UT	330	7.93	0.7803E+12
29	15:10:05UT	339	12.44	0.1922E+13
30	10:15:06UT	395	10.60	0.1394E+13
30	11:15:06UT	409	11.14	0.1541E+13

Table 1: The ionosonde measurements of hmf2, Nmf2 and fof2 values for Addis Ababa station in 2014 for three days in May month.

The knowledge about the density profile of the topside ionosphere remains poor. To overcome this limitation, many innovative techniques have been applied to estimate the topside density. Analytical Modeling using mathematical functions like exponential, parabolic, Epstein and Chapman functions etc have been done to estimate the topside profile. The Chapman function is simple and has great potential to fits the topside ionospheric profile well up to several hundred kilometers above the F2-peak. They used the approximation that the scale height above the peak of the F2 layer is constant and equal to the Chapman scale height at the height of F2 layer peak density (hmF2). Using this constant scale height the topside profile was reconstructed. Since this method uses only bottom side information and with no information from the top side, the derived profiles. As we can see from figure 13 the first panels is the Chapman production function and the second one the over all plot of ionogram electron density profile. The Chapman model is used to estimate the topside electron density by using the bottom side information from F2-peak. The reflectivity of the Chapman electron density is depends on the solar zenith angle and the scale height. The second one is the electron density measured by the ionogram. This electron density is reflected around 100 km in E-layer and up to the F2 peak and below the Elayer that mean at D-layer the absorption is dominate than reflection. The disadvantage of ionosonde is it measures only the bottom side electron density to the F2-peak and omitted the information above the F2-peak.

4. Conclusion

Inthisstudy, we delved into the working so Ionosonde and its measurement techniques, with a particular focus on electron density as the fundamental parameter shaping ionospheric properties. Electron density profiles, which peak within the altitude range of 150-350 km, were scrutinized. Ionosonde measurements captured electron density reflections from the E-layer to the F2 peak, while absorption was noted below the E-layer, particularly within the D-layer.

Keyiono spheric parameters including electron density profile (Ne), maximum electron density (NmF2), maximum ionization height (hmF2), and critical frequency (foF2) were instrumental in our analysis. However, it's worth noting that Ionosonde's reach is limited to the lower ionospheric region, as evidenced by our results. To compensate for this limitation, we employed the Chapman electron density profile to extend our observations to the upper ionospheric layers.

Our findings, based on data from the Addis Ababa station in 2014, underscore the significance of considering diurnal variations, particularly evident in the Chapman model's depiction of maximum electron density during noon or periods of minimal solar zenith angles. Nevertheless, it's imperative to acknowledge the constraints imposed by data availability and the need for further.

exploration to enhance our understanding of ionospheric Bilitza, D., 2008. The importance of bottomside and topside sounding dynamics.

measurements for the development of iri, in: AIP Conference Pro-ceedings, American Institute of Physics. pp. 9–19. Chartier, A.T., Smith, N.D., Mitchell, C.N., Jackson, D.R., Patilongo,

Acknowledgment

P.J., 2012. The use of ionosondes in gps ionospheric tomography at The authors gratefully acknowledge the Washera Geo space low latitudes. Journal of Geophysical Research: Space Physics 117. and Radar Science Research Laboratory in the Department of Physics at Bahir Dar University and Bonga
University.

Funding

The authors received no direct funding for this work.

Author Details

Amsalu Hundessa Dinede E-mail: amse2022amse2014@gmail.com or amesalu062@gmail.com
Tel:+251927601301

Washera Geo space and Radar Science Research Laboratory, Bahir Dar, Ethiopia. Department of Physics and College of Science, Bonga University, Bonga, Ethiopia.

Disclosure Statement

The authors declare that they have no known competing financial interests or personal relationships that could have influenced the work reported in this study.

References

1. Barona Mendoza, J. J., Quiroga Ruiz, C. F., & Pinedo Jaramillo, C. R. (2017). Implementation of an Electronic Ionosonde to Monitor the Earth's Ionosphere via a Projected Column through *USRP. Sensors,* 17(5), 946.
2. Belehaki, A., Jakowski, N., & Reinisch, B. W. (2003).

Comparison of ionospheric ionization measurements over Athens using ground ionosonde and GPS-derived TEC values. *Radio Science, 38*(6), 13-1.
3. Di Giovanni, G., & Radicella, S. M. (1990). An analytical model of the electron density profile in the ionosphere. *Advances in Space Research, 10*(11), 27-30.
4. Fang, H., Hongqiao, H., Huigen, Y., Beichen, Z., Dehong, H., Yonghua, L., ... & Jianjun, L. (2016). Recent progress in Chinese polar upper-atmospheric physics research: review of research advances supported by the Chinese Arctic and Antarctic expeditions. *Advances in Polar Science, 27*(4), 219-232.
5. Forsythe, V. V., Azeem, I., Blay, R., Crowley, G., Makarevich, R. A., & Wu, W. (2021). Data assimilation retrieval of electron density profiles from ionosonde virtual height data. *Radio Science, 56*(5), 1-15.
6. Garcıa-Fernández, M., Hernandez-Pajares, M., Juan, J. M., Sanz, J., Orús, R., Coisson, P., ... & Radicella, S. M. (2003). Combining ionosonde with ground GPS data for electron density estimation. *Journal of atmospheric and solar-terrestrial physics, 65*(6), 683-691.
7. Horwitz, J. L., Comfort, R. H., Richards, P. G., Chandler, M. O., Chappell, C. R., Anderson, P., ... & Brace, L. H. (1990). Plasmasphere-ionosphere coupling: 2. Ion composition measurements at plasmaspheric and ionospheric altitudes and comparison with modeling results. *Journal of Geophysical Research: Space Physics, 95*(A6), 7949-7959.
8. Huang, X., & Reinisch, B. W. (2001). Vertical electron content from ionograms in real time. *Radio Science, 36*(2), 335-342.
9. Ma, X. F., Maruyama, T., Ma, G., & Takeda, T. (2005). Three-dimensional ionospheric tomography using observation data of GPS ground receivers and ionosonde by neural network. *Journal of Geophysical Research: Space Physics, 110*(A5).
10. McNamara, L. F., Baker, C. R., & Decker, D. T. (2008). Accuracy of USU-GAIM specifications of foF2 and M (3000) F2 for a worldwide distribution of ionosonde locations. *Radio Science, 43*(01), 1-10.
11. Reinisch, B. W., Huang, X. Q., Belehaki, A., Shi, J. K., Zhang, M. L., & Ilma, R. (2004). Modeling the IRI topside profile using scale heights from ground-based ionosonde measurements. *Advances in Space Research, 34*(9), 2026-2031.
12. Rishbeth, H., & Garriott, O. K. (1969). Introduction to ionospheric physics. Introduction to ionospheric physics.
13. Souza, A. L. C. D., & Camargo, P. D. O. (2019). Comparison of GNSS indices, ionosondes and all-sky imagers in monitoring the ionosphere in brazil during quiet and disturbed days. *Boletim de Ciências Geodésicas, 25,* e2019s005.
14. Stankov, S. M., Jakowski, N., Heise, S., Muhtarov, P., Kutiev, I., & Warnant, R. (2003). A new method for reconstruction of the vertical electron density distribution in the upper ionosphere and plasmasphere. *Journal of Geophysical Research: Space Physics, 108*(A5).
15. Tsai, L. C., Liu, C. H., & Hsiao, T. Y. (2009). Profiling of ionospheric electron density based on FormoSat-3/COSMIC data: results from the intense observation period experiment. *Terrestrial, Atmospheric and Oceanic Sciences, 20*(1), 181.
16. Warrington, E. M., Zaalov, N. Y., Naylor, J. S., & Stocker, A. J. (2012). HF propagation modeling within the polar ionosphere. *Radio Science, 47*(04), 1-7.
17. Yamashita, C. S. (1999). Efeito das tempestades magnéticas intensas na ionosfera de baixa latitude. São José dos Campos. 75p. Dissertação de Mestrado em Geofísica Espacial, *Instituto Nacional de Pesquisas Espaciais.*